Novel layered silicate and microporous silica materials in the Na-magadiite–H_2O–$(TMA)_2O$ system

Fathi Kooli,* Yoshimichi Kiyozumi and Fujio Mizukami*

National Institute of Advanced Industrial Science and Technology (AIST), Tsukuba Central 5, 1-1-1 Higashi, Tsukuba, Ibaraki 305-8565, Japan. E-mail: f-mizukami@aist.go.jp

Received (in Montpellier, France) 1st June 2001, Accepted 17th September 2001
First published as an Advance Article on the web

Novel layered silicate and microporous silica materials have been successfully synthesized in a Na-magadiite–H_2O–$(TMA)_2O$ system. At appropriate water and TMAOH contents, Na-magadiite was converted into a new layered silicate phase (KLS2) at relatively low temperatures, in the range 130 to 150 °C. However, a microporous silica material (FLS) was formed at higher temperatures, from 160 up to 180 °C. The samples were characterized by powder X-ray diffraction, ^{29}Si magic-angle spinning NMR, infra-red spectroscopy, scanning electron microscopy, thermogravimetric and differential thermal analysis, and adsorption measurements. It was found that the KLS2 phase has lower thermal stability than the FLS phase. An amorphous phase was formed upon heating KLS2 below 300 °C, while FLS was found to be stable up to 600 °C and exhibits a surface area of 300 $m^2\ g^{-1}$ and micropore volume of 0.082 mL (liquid nitrogen) g^{-1}. Factors such as the Na-magadiite, TMAOH and water contents, which dominate the conversion of Na-magadiite, are discussed.

Hydrous layer sodium silicates (makatite, kenyaite, magadiite, kanemite) are minerals that exhibit a rich intercalation chemistry and are easily synthesized under hydrothermal conditions.[1,2] Much work has been devoted to the resolution of the crystal structure of such minerals[3–5] and to the design of catalysts and/or adsorbents by various intercalation procedures.[6–8] Magadiite has reactive silanol groups in its interlayer space;[9] organic groups can be grafted to these groups by reaction with organochlorosilanes, modifying the interlayer space. The grafted organic groups enable the formation of novel layered silicate–polymer nanocomposites.[10,11]

Synthesis of highly ordered mesoporous materials from layered polysilicate kanemite has been reported.[12] The synthesis procedure used is based on the interaction of the flexible layered silicate with long-chain alkylammonium cations such as hexadecyltrimethylammonium ions (C_{16}-TMA^+).[13] The silicate layers of kanemite are reorganized due to the ability of the surfactant molecules to change from a bilayered structure to a cylindrical micelle-like aggregate.[14] Studies have also been reported concerning the use of short-chain alkylammonium cations, such as tetrapropylammonium (TPA^+) and tetrabutylammonium (TBA^+), to prepare the corresponding zeolites from layered silicates.[15–17] The tetramethylammo- nium (TMA^+) cation is an interesting component in such hydrothermal syntheses, because it is used as a structure-directing agent alone or together with certain other cations in preparing a variety of molecular sieves that exhibit variations in framework composition and structure.[18] Tetramethylammonium hydroxide (TMAOH) has also been used to synthesize silicate hydrates from a mixture of silica, water and cationic organic molecules.[19] These silicate hydrates are reported to be useful model systems for studying zeolites synthesis[20] and the nucleation of high-silica zeolites.[21] Hydrothermal treatment of the mixture SiO_2–NaOH–H_2O–TMAOH–1,4-dioxane resulted in a new silicate layered structure with helical morphology (HLS phase). The organic solvent was essential for such a phase and morphology to be obtained.[22] The structure is composed of layers having cups of half sodalite cages facing up and down in alternating fashion. TMA ions are incorporated into the cup-shaped cages and Na and H_2O molecules are located between two silicate layers.[23] Recently, we have converted a protonated magadiite to a new microporous silica phase using TMA cations as directing agents, in the absence of 1,4-dioxane.[24] In the present work, we have synthesized new materials from Na-magadiite and TMA cations, without the use of organic solvent. Detailed product characterization and synthesis conditions are described in order to identify a possible mechanism of the Na-magadiite conversion.

Experimental

Synthesis

Na-magadiite (SKS-2 supplied by Clariant, Japan; 1 g) was mixed with 0.5 g of deionized water and 2.3 g of TMAOH solution (15% w/w). The reaction mixture was heated statically in Teflon-lined autoclaves under various conditions. The resulting product was recovered by centrifugation, washed with acetone and dried at 40 °C overnight.

The effect of TMAOH, water and silica content was examined separately, while keeping the other contents constant for a given reaction period of 5 days at different temperatures.

Exchange of Na cations in the KLS2 phase with various C_n-TMA cations was prepared by dispersing 0.5 g of the solid in 10 cm^3 of an aqueous solution of the cations (0.5 mol dm^{-3}) at room temperature overnight. The product was filtered, washed with 150 cm^3 of deionized water and dried in air at 40 °C.

Calcination of the obtained products was performed in air at different temperatures from 300 to 800 °C for 10 h; the heating rate was 3 °C min^{-1}.

DOI: 10.1039/b104831g

Characterization

Powder XRD patterns were obtained with an MXP 18 diffractometer (Mac-Science Co., Ltd) using Cu-Kα radiation ($\lambda = 0.15418$ nm). C, H, N analyses were performed using a CE Instruments model EA 1110 CHN analyzer. An inductively coupled plasma (ICP) spectrophotometer (model SII 1700HVR) was used for elemental analysis of Si and Na. Thermogravimetry (TG) and differential thermal analysis (DTA) were performed using a Mac-Science TG-DTA 2000 analyzer; all samples were heated to 1000 °C at a heating rate of 5 °C min^{-1}.

Solid state ^{29}Si MAS NMR spectra were recorded at room temperature on a Bruker AMX 500 solid NMR spectrometer. A delay time of 800 s was applied between pulses and a total of 25 to 70 scans were recorded for each sample. The chemical shift was referenced with respect to the ^{29}Si signal of hexamethyldisiloxane (HMDS). Integration of the signals in the ^{29}Si spectrum was achieved by deconvolution using GRAMS-32 software.

FTIR spectra of samples were recorded in air on a BIORAD FTS-45RD spectrometer (in the range 400–4000 cm^{-1}) using the KBr pressed-pellet technique. Morphologies of products were examined by scanning electron microscopy (SEM) using a Hitachi S-800 electron microscope. Nitrogen adsorption isotherms were measured at liquid nitrogen temperature on a Belsorp 28 SP instrument. All samples were outgassed at 200 °C and 10^{-3} Pa for 2 h prior to the adsorption measurements.

Results and discussion

Synthesis

The choice of the TMA cation as a template for the conversion of Na-magadiite was not fortuitous. Based on the literature,[18c] TMA cations operate mainly to direct the crystallization of silica to a sodalite structure. Conversion of Na-magadiite was studied by varying the reaction temperature and time.

Effect of reaction temperature. Fig. 1 shows powder XRD patterns of as-received Na-magadiite and products of the conversion reaction performed at different temperatures for 5 days. Na-magadiite exhibits a basal spacing of 1.53 nm, which agrees with values reported previously for synthetic and natural magadiite.[25–27] At low reaction temperatures such as 100 °C, Na-magadiite was partially intercalated by TMA cations and an increase in basal spacing to 1.80 nm was observed. In the temperature range 130 to 150 °C, however, Na-magadiite was converted to a new phase (denoted KLS2), which bore some similarity to KLS1 prepared in the presence of 1,4-dioxane.[28] Further increases in temperature into the range 160 to 180 °C leads to formation of another new phase (denoted FLS) similar to that reported from H-magadiite.[24] In addition, a quartz phase was also detected in the reaction at 180 °C. This phase was mainly formed at higher reaction temperatures (190 °C). Table 1 gives the *d* spacing and the relative intensities for the major peaks in the powder XRD patterns of the KLS2 and FLS phases.

Effect of crystallization time. Fig. 2 shows powder XRD patterns of products from the conversion reaction of Na-magadiite performed at 150 °C for different reaction times. The FLS phase was formed following a reaction time of 3 days, while a powder XRD pattern indicative of the KLS2 phase was obtained only after a reaction time of 5 days. The latter phase was not stable for reaction times longer than 5 days. In fact, characteristic reflections of the FLS phase reappeared with low relative intensity after 10 days reaction. After 30 days FLS became the main crystalline product. Longer reaction times of approximately 60 days resulted in the formation of FLS and quartz at the expense of the KLS2 phase.

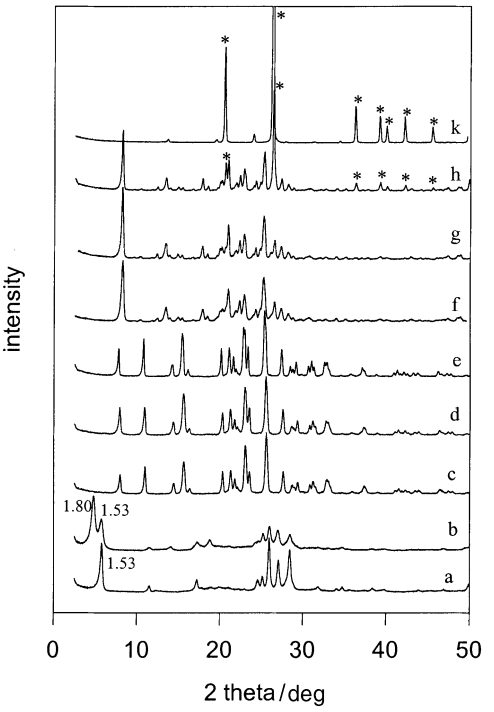

Fig. 1 Powder XRD patterns of Na-magadiite (1 g, a) reacted with TMAOH (2.3 g) and water (0.5 g) at different temperatures: (b) 100, (c) 130, (d) 140, (e) 150, (f) 160, (g) 170, (h) 180 and (k) 190 °C. * Peaks correspond to silica phases.

A higher reaction temperature of 170 °C favors the conversion of Na-magadiite to the FLS phase after a shorter reaction time (1 day), compared to the reaction at 150 °C. Quartz was detected after 10 days of reaction. The proportion of quartz

Table 1 Powder XRD data for the different phases formed from Na-magadiite

KLS2		FLS		FLS (500)[a]	
d/Å	Rel. int.	*d*/Å	Rel. int.	*d*/Å	Rel. int.
11.354	43	10.179	100	9.148	100
0.818	58	8.095	5	8.330	8
6.188	19	6.867	7	6.846	62
5.741	66	6.347	21	6.120	15
5.487	12	6.154	7	5.507	8
4.401	44	5.734	8	4.599	10
4.207	45	5.569	7	4.449	22
4.107	31	4.823	21	4.358	18
4.039	12	4.691	9	4.103	16
3.893	75	4.354	16	3.890	22
3.864	71	4.267	20	3.821	24
3.801	46	4.133	52	3.677	13
3.506	100	3.983	17	3.432	51
3.247	42	3.897	33	3.319	26
3.131	17	3.798	41	3.247	21
3.101	13	3.645	10	3.064	8
3.060	23	3.587	21		
2.915	17	3.528	17		
2.877	25	3.460	69		
2.851	16	3.297	33		
2.742	23	3.206	20		
2.720	23	3.103	14		
2.506	6				
2.420	15				
2.182	11				

[a] FLS phase calcined at 500 °C.

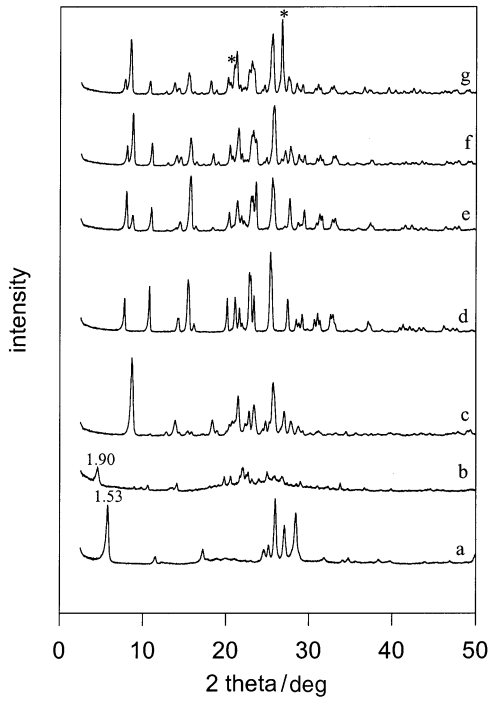

Fig. 2 Powder XRD patterns of (a) Na-magadiite and resulting products after reaction with TMAOH and water, at 150 °C for different reaction times: (b) 1, (c) 3, (d) 5, (e) 10, (f) 30 and (g) 60 days. * Peaks correspond to silica phases.

increased in the product produced at higher temperatures and it was detected at relatively shorter reaction times, for example 1 day at 190 °C.

Effect of TMAOH content. Increasing the amount of template to more than 2.3 g favors the conversion of Na-magadiite to the KLS2 phase at 150 °C. Lower amounts of TMAOH (1 g) led to the formation of the FLS phase, which was partially converted to the KLS2 phase by increasing the amount of TMAOH added up to 1.3 g. Amounts of TMAOH higher than 3.5 g switches the conversion of Na-magadiite to a sodalite phase.

By increasing the recrystallization temperature to 170 °C and the amounts of TMAOH up to 5 g Na-magadiite was transformed to KLS2, as a result of conversion of FLS to KLS2. Quartz was obtained when 7.5 g of TMAOH was added. However, at 180 °C, the conversion of Na-magadiite to the FLS phase was achieved independently of the amount of TMAOH added, up to 5 g.

Effect of water content. The conversion of Na-magadiite to the KLS2 phase at 150 °C was achieved in a very narrow range of water content from 0 to 0.5 g. Increasing the amount of water, up to 5 g, switches the product from KLS2 to FLS. The transformation of Na-magadiite was difficult to achieve when more than 10 g of water was used and Na-magadiite remained the main crystalline phase.

At a crystallization temperature of 170 °C, Na-magadiite was converted to crystalline FLS in a large range of water contents from 0.5 g up to 10 g. For further increases of water content, TMA cations were intercalated between the magadiite layers with traces of the FLS phase also being formed.

Effect of silicon content. Powder XRD patterns indicated that the KLS2 phase was formed when the amount of Na-magadiite added was approximately 1 g to TMAOH (2.3 g) and H_2O (0.5 g). Quartz was formed with lower amounts of Na-magadiite. However, mainly FLS was detected, with traces of KLS2, when 2 g of Na-magadiite was added to the reaction mixture.

Table 2 Chemical analysis of different phases obtained under different conditions

Samples[a]	Si/Na[b]	%C	%H	%N	$\%H_2O$[c]
Na-magadiite	7.10				13.10
100 °C (5 days)	14.02	5.64	2.54	1.42	9.21
130 °C (5 days)	6.28	10.48	4.19	2.86	10.12
150 °C (5 days)	5.94	10.04	4.12	2.80	12.22
170 °C (5 days)	133.42	7.72	2.25	2.09	1.21
190 °C (5 days)	288.00	0.42	0.08	0.04	0.21
150 °C (1 day)	17.34	11.90	3.95	2.90	26.61
150 °C (3 days)	232.00	8.04	2.01	2.04	2.03
150 °C (5 days)	5.94	10.04	4.12	2.80	12.20
150 °C (10 days)	11.20	10.94	4.10	2.96	10.44
150 °C (30 days)	15.27	8.77	3.07	2.39	5.03
150 °C (60 days)	20.64	7.54	2.00	1.60	3.14

[a] 100 °C (5 days) means that the conversion reaction was performed at 100 °C for a duration of 5 days. [b] Molar ratio. [c] Deduced from the TG analysis in the 25–200 °C temperature range.

Characterization

Chemical analysis. Table 2 presents the molar ratio Si/Na and CHN analyses of the different phases prepared under different conditions. The water content is also reported.

The Si/Na molar ratio of the solid products depends on the nature of the phases formed. KLS2 phases are rich in Na cations compared to FLS products, in which only trace amounts of Na cations are detected. In addition, Si/Na in the KLS2 phase is lower compared to the Na-magadiite precursor and to KLS1 materials.[28] This decrease is due to partial dissolution of silicate layers during the recrystallization of the KLS2 phase. At a set temperature of 150 °C, the Si/Na molar ratio increases with reaction times over 5 days, indicating a lesser reactivity of Na cations at longer times. The amount of organic moieties present in the products decreases gradually as the recrystallization temperature increases from 130 to 170 °C, however it was significantly reduced at 190 °C. The low amount of carbon in the material prepared at 100 °C is due to incomplete exchange of Na by TMA cations. These data indicate that the KLS2 phase contains more TMA cations than the FLS material. From the CHN analyses of the KLS2 and FLS phases, a C/N molar ratio of about 4.15 was determined, indicating that TMA cations are incorporated intact in the as-synthesized materials.

Thermal properties. TG and DTA curves of Na-magadiite and the different phases synthesized at 150 °C for different reaction times are illustrated in Fig. 3. The TG and DTA profiles of the precursor are similar to those previously reported.[6] After reaction with TMAOH and water for 1 day, the TG profile shows two mass losses totalling 26.6% of the initial weight. These are associated with release of physically bound and intercalated water molecules, accompanied by two endothermal peaks in the DTA at 50 and 220 °C, respectively. A third mass loss of 7.5%, recorded at temperatures above 250 °C, corresponds to combustion of TMA cations and is associated with an exothermal peak at 420 °C with a shoulder at 340 °C in the DTA. The TG profile of the FLS phase shows predominantly one mass loss of 14% in the temperature range 250 to 500 °C, corresponding to thermal decomposition of TMA cations, and is accompanied by an exothermal peak centered at 460 °C in the DTA. The continuing mass losses at temperatures higher than 500 °C are probably a result of slow desorption of decomposed residues. The decomposition temperature of TMA cations in the FLS phase is higher compared to the corresponding process in an FLS1 phase prepared from H-magadiite (420 °C).[24] A continuous mass loss, extending

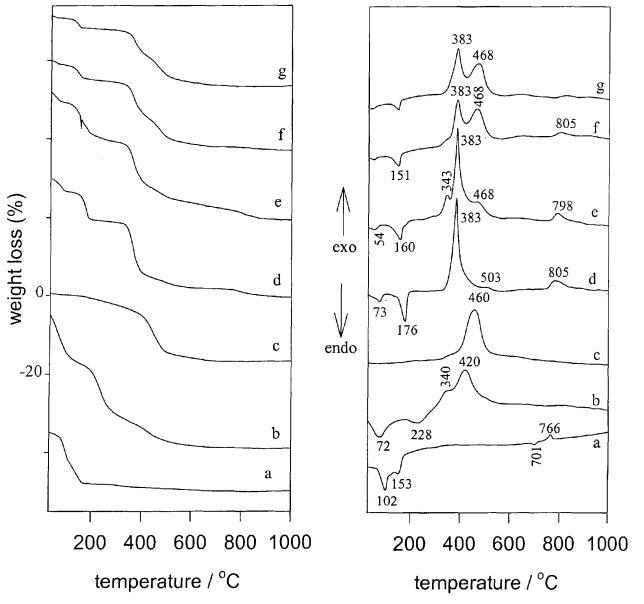

Fig. 3 TG (left) and DTA (right) traces of (a) Na-magadiite and (b–g) the resulting phases obtained after reaction at 150 °C for different reaction times. See Fig. 2 for details.

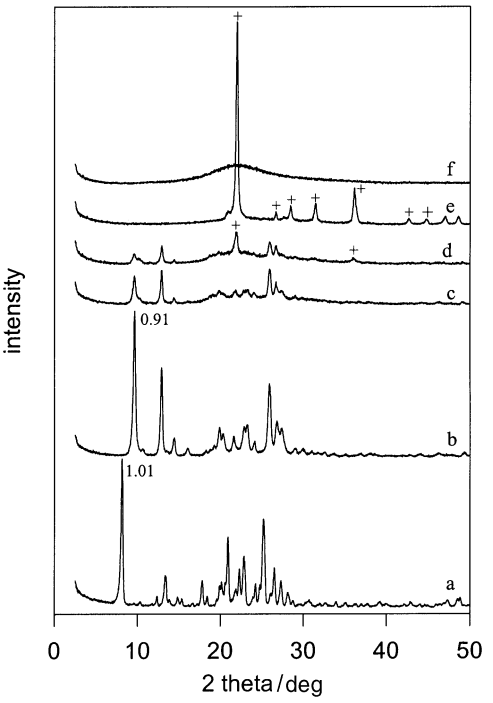

Fig. 4 Powder XRD patterns of FLS calcined at different temperatures: (a) as-synthesized, (b) 500, (c) 600, (d) 700, (e) 800 °C. (f) corresponds to KLS2 phase calcined at 500 °C. + Peaks correspond to the cristobalite phase.

from room temperature up to 250 °C, totalling 2% is assigned to loss of physiadsorbed water molecules and eventually some structural water. This behavior is typical for a hydrophobic high-silica zeolite that contains very small amounts of water and has narrow pore openings.[29]

The TG profile of the KLS2 phase shows three general regions of mass loss, corresponding to the removal of physiadsorbed water, molecules of water coordinated to Na cations, and to the elimination and combustion of TMA cations.[23,28] A fourth mass loss was also detected at higher temperatures, in the range 780 to 820 °C, which could be related to the oxidation of carbonaceous residues and their subsequent release as carbon dioxide.[30] The first two mass losses are determined from DTA to be two endothermic effects with minima at about 60 and 160 °C. The exothermic peaks at 383 and 805 °C correspond to combustion of organic cations and carbonaceous residues. The combustion temperature of TMA cations (460 °C) in the FLS phase is higher compared to that in the KLS2 phase (386 °C), indicating that the TMA cations are in different environments in the two materials. For longer reaction times, the mass losses related to the different types of water molecules and to combustion of TMA cations decrease. A new exothermal effect at 468 °C appears and its intensity increases with increasing reaction time, due to the presence of FLS. At the same time, the intensity of the exothermal peak at 383 °C decreases, indicating some conversion of KLS2 to FLS.

From the chemical analysis and mass losses, the empirical formula of the FLS product is $H_{0.065}SiO_{2.1}(TMA)_{0.135}\cdot 0.08H_2O$ and that of the KLS2 material is $H_{0.4}Na_{0.17}SiO_{2.4}(TMA)_{0.22}(H_2O)_{0.57}$.

The elimination of water coordinated to Na cations and dehydroxylation of the KLS2 phase below 300 °C results in the collapse of the layered structure, and an amorphous product was obtained. Note that the amorphization occurs even before the removal of TMA cations (Fig. 4). However, the framework structure of FLS was found to be stable after calcination at 500 °C, and a new phase was obtained with a shift of *d* spacing to low values. This shift is related to the elimination of TMA cations and to the lattice deformation of the Si–O network. The FLS phase partially collapses at higher temperatures, such as 700 °C, with amorphous silica being formed, and cristobalite was formed at a calcination temperature of 800 °C (see Fig. 4).

Table 1 presents the *d* spacing and relative intensities of the major peaks in the powder XRD pattern for the FLS phase calcined at 500 °C.

NMR data. ^{29}Si MAS NMR spectra for the precursor Na-magadiite and products from the reaction at 150 °C for different durations are shown in Fig. 5. Na-magadiite exhibits two general Si environments, namely Q^3-type $HOSi(OSi)_3$ or $Na^+[OSi(OSi)_3]$ sites centered at −99.0 ppm, and Q^4-type $Si(OSi)_4$ sites with multiple signals at −110.1, −111.1 and

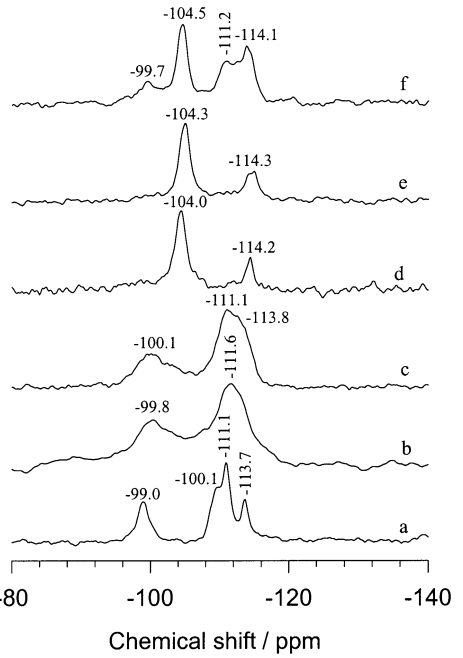

Fig. 5 ^{29}Si MAS NMR spectra of (a) Na-magadiite and (b–f) resulting phases obtained after reaction at 150 °C for different times. See Fig. 2 for details.

−113.7 ppm,[6] with a Q^3/Q^4 ratio of 0.35. After 1 day of reaction, the ^{29}Si MAS NMR spectrum shows two broad signals at −99.8 and −111.6, assigned to Q^3 and Q^4 Si types. The Q^3/Q^4 ratio is almost the same as that measured for the precursor material, which could indicate that the structure of the silicate layer was unchanged. The broadness of the Si peaks is most probably due to the low crystallinity of the product. A similar ^{29}Si spectrum was obtained after the reaction of Na-magadiite for 3 days, with a Q^3/Q^4 ratio of 0.26, indicating that the FLS phase is rich in the Q^4-type silicon and that it has similar short-order structure with broadened signals compared to the starting magadiite. However, after reaction times of 5 to 10 days, the ^{29}Si MAS NMR spectrum of the KLS2 phase is different from that of the FLS one, with a decreased intensity of the Q^4 signal (−114.2 ppm) and an increase in the intensity of the Q^3 signal (−104.0 ppm). This suggests that the structure of the silicate layer has completely changed and that the KLS2 phase is rich in Q^3-type silicon. The value of the Q^3/Q^4 ratio for KLS2 is about 3.93 and close to that reported for HLS[23] and KLS1 materials.[28] The sharpness of the peaks in the ^{29}Si MAS NMR spectrum of the KLS2 phase also indicates an increase in the crystallinity compared to the starting precursor. These facts suggest that the conversion of Na-magadiite to the KLS2 phase occurs through dissolution of the silicate layers and with significant Si−O−template or Si−O−H linkages being formed in the final product. The ^{29}Si MAS NMR spectrum shows characteristic signals of both KLS2 and FLS phases, resulting from the presence of the two different materials, for reaction times longer than 30 days. The signals of the latter phase increase and those of KLS2 decrease considerably for further increases in of reaction time up to 60 days (not shown).

Infra-red spectroscopy. Infra-red spectroscopy yields valuable information concerning the framework of the new phases. This technique has been successfully employed in the study of zeolite framework characteristics.[31] The FT-IR spectra for Na-magadiite and reaction products at 150 °C for different reaction times are shown in Fig. 6. The mid FT-IR spectrum for Na-magadiite agreed well with those reported elsewhere.[27,32,33] After 1 day of reaction, two new bands at 1487 and 947 cm^{-1}, related to intercalated TMA cations, were observed. The magadiite absorption bands in the 1500−400 cm^{-1} range are almost unchanged, although some broadening of the bands is observed. Thus, the framework structure of layered silicate is not changed during the intercalation process, in agreement with the ^{29}Si MAS NMR data. A shift of the ν(Si−O$^-$) stretching vibrations in the region 1100−1050 cm^{-1} is also observed. The FT-IR spectrum of the FLS phase (obtained after 3 days of reaction) is similar to that reported for the FLS2 one.[24] The bands at 1235 and 1157 cm^{-1} are assigned at the empirical level to asymmetric stretching vibrations of Si−O−Si, characteristic of five-membered rings in zeolites.[34] The band at 806 cm^{-1} is attributed to ν_{sym}(Si−O−Si) while the band at 602 cm^{-1} could be ascribed to the "crystallinity peak" in zeolite synthesis, resulting from the formation of silica five-membered rings during hydrothermal treatment.[35,36] In the case of the as-synthesized KLS2 phase, the characteristic bands of TMA cations are also observed at 1487 and 952 cm^{-1}. However, the band at 952 cm^{-1} coalesces into a second peak at 941 cm^{-1} as the KLS2 phase is formed [compare Fig. 6(c) and (d)]. The latter is assigned to the Si−O stretching vibrations of Si−O−H linkages.[37] Various other possible assignments are given to this band in the literature.[38] The band at 1157 cm^{-1} is enhanced and assigned, along with the band at 1068 cm^{-1}, to an asymmetric stretching vibration, ν_{as}(Si−O− Si). The symmetric stretching mode of the Si−O−Si chain corresponds to the band at 760 cm^{-1}. The absorptions at 650−550 cm^{-1}, on the other hand, have been assigned previously to the presence of a double-ring of tetrahedra in the zeolitic framework.[39] The intensity ratio of the peak at 548 cm^{-1} to the one at

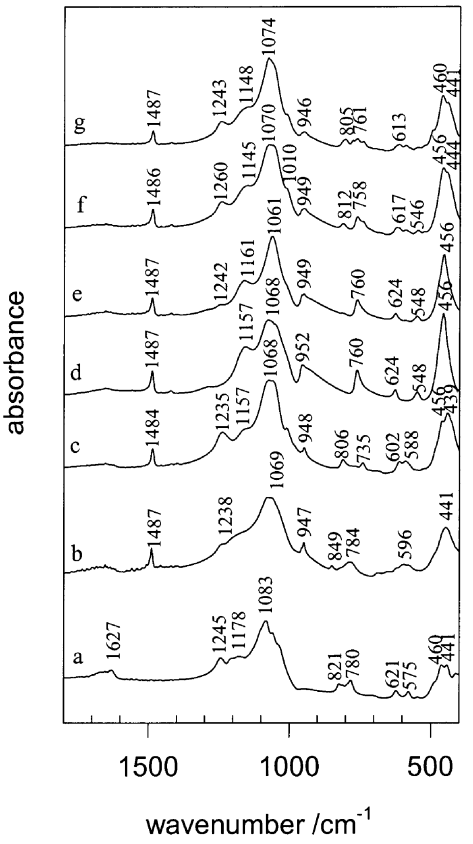

Fig. 6 FT-IR spectra of (a) Na-magadiite and of (b−g) resulting phases presented in Fig. 2.

456 cm^{-1} is often used as a quantitative measurement of zeolite crystallinity.[40] The band at approximately 456 cm^{-1} is assigned to the Si−O−Si bending mode.[31]

The FT-IR spectrum of the product from the reaction for a period of 10 days exhibits similar overall characteristics to those of the KLS2 phase, with traces of bands related to the FLS phase. The characteristic bands of the latter phase are clearly enhanced at longer recrystallization times; meanwhile the bands related to the KLS2 product decrease in intensity.

SEM observations. The characteristic morphological changes of Na-magadiite recrystallized at different reaction times and at a set temperature of 150 °C are shown in Fig. 7. Na-magadiite is known to adopt a particle morphology composed of silicate layers intergrown to form spherical nodules resembling rosettes.[27] The scanning electron micrograph obtained after reaction for 1 day shows the presence of two phases, one related to magadiite intercalated with TMA cations and the other a phase with needle-shaped crystals. The needles are 50 nm in length. The population of needles in the product increases after two days' reaction with a concomitant decrease in their length. The needle habit totally disappears for a recrystallization period of 3 days, and well-developed platelets are formed. Thus, the FLS phase nucleated and grew from needles or fibers to crystallite platelets. However, the morphology of the KLS2 phase consists of small cubic crystallites with a dimension of 1 nm, stacked adjacent to each other. For a longer crystallization time of 30 days the original stack of crystallites is apparently not preserved and the SEM micrograph (not shown) reveals loosely compacted assemblages of platelets.

Due to the assumed layered habit of the as-synthesized KLS2 phase, it appeared reasonable to attempt ion exchange of the Na cations with different alkylammonium cations.[9] Indeed, the basal spacing of KLS2 is expanded by the alkylammonium cations and shows a systematic increase as the

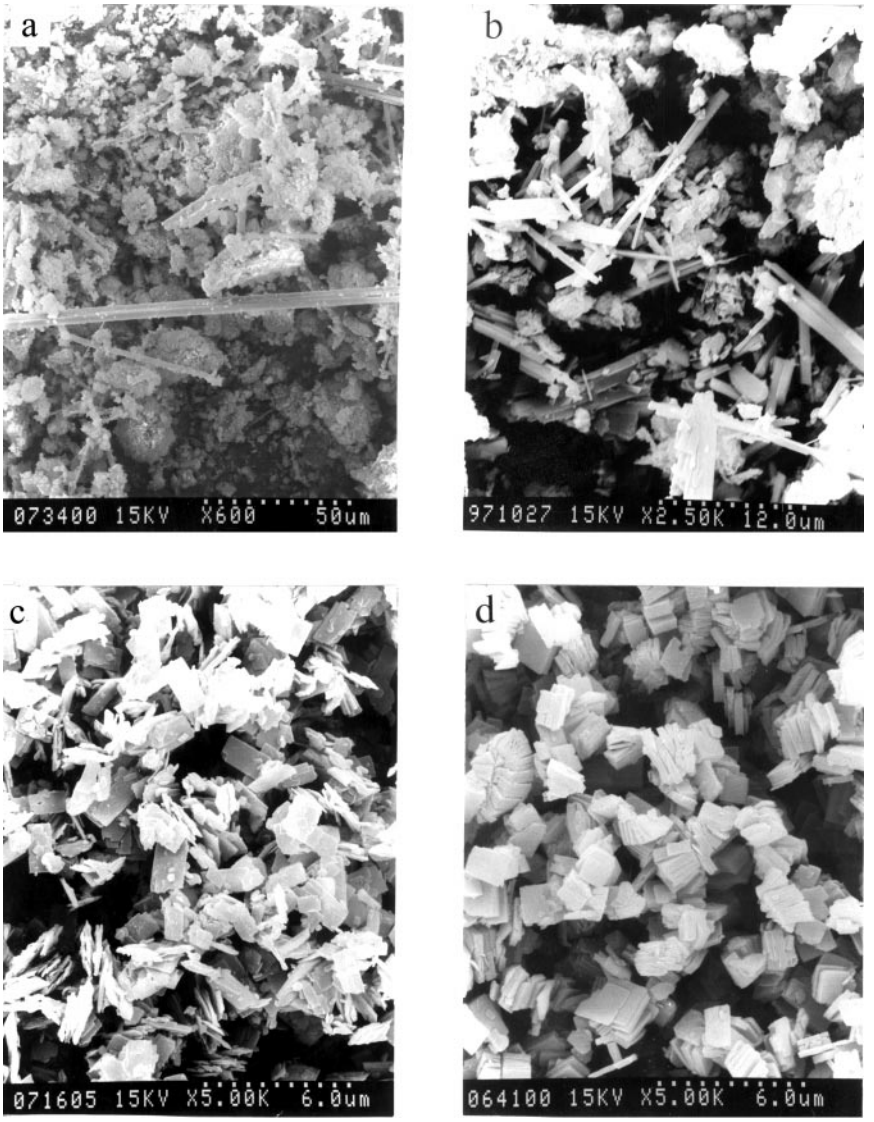

Fig. 7 SEM micrographs of Na-magadiite converted in the water–TMAOH system at 150 °C for different times: (a) 1, (b) 2, (c) 3 and (d) 5 days.

number of carbon atoms in the alkyl chain increases. These data confirm the layered structure of the KLS2 material.

Surface area and microporosity. Representative nitrogen adsorption isotherms of the Na-magadiite, KLS2 and FLS materials, calcined at 500 °C, are presented in Fig. 8 The shape of the isotherm for the calcined Na-magadiite and KLS2 materials corresponds to type IV in the IUPAC classification,[41] being characteristic of non-porous materials. For the calcined FLS material, however, the shape of the isotherm, which has a small hysteresis loop, corresponds to type I, thus indicating a microporous character.[41] The shape of this isotherm is similar to that reported for zeolite materials.[42]

Specific surface areas of the calcined materials, estimated on the basis of the BET equation, are collected in Table 3. The corresponding BET constants (C_{BET}) are also listed in Table 3. The specific area of the calcined FLS material is larger than that of the calcined Na-magadiite and KLS2 phases. The low surface areas observed for the latter phases are most probably due to collapse of the layered structure. However, in the case of the FLS material, the increase of surface area upon calcination can be attributed to the formation of micropores.

The calcined Na-magadiite and KLS2 phases, having low surface areas, give a positive C_{BET}. However, the calcined FLS material gives a negative C_{BET}. According to the BET theory, C_{BET} is related exponentially to the enthalpy (heat) of adsorption on the first adsorbed layer. A negative value for C_{BET} has no physical meaning, indicating that the BET method is not suitable for the calculation of the specific surface area of these materials with primary micropore filling.[43] We have used another method, therefore, to calculate the micropore volume and external surface area of calcined FLS materials, which has been recently applied to pillared clays and titanates.[44,45] This procedure corresponds to subtraction of the amount of N_2 adsorbed on micropores from the total experimental isotherm. The modified isotherm should give a good correlation coefficient and positive C_{BET}. Table 3 reports the external surface areas and micropore volumes determined by this method. The micropore volume of the calcined FLS phase (prepared at 170 °C) is approximately 0.082 mL (liquid nitrogen) g^{-1}. This value is lower than that reported for similar calcined phases prepared from protonated magadiite[24] and other zeolite materials.[42]

Reaction mechanism

A plausible reaction mechanism for the formation of the KLS2 phase is thus proposed: Na-magadiite is intercalated with TMA cations in the first stage, then TMA-intercalated magadiite is transformed into the KLS2 phase. This conversion proceeds through a transition FLS phase free from Na cations. This intermediate phase was not detected when 1,4-dioxane

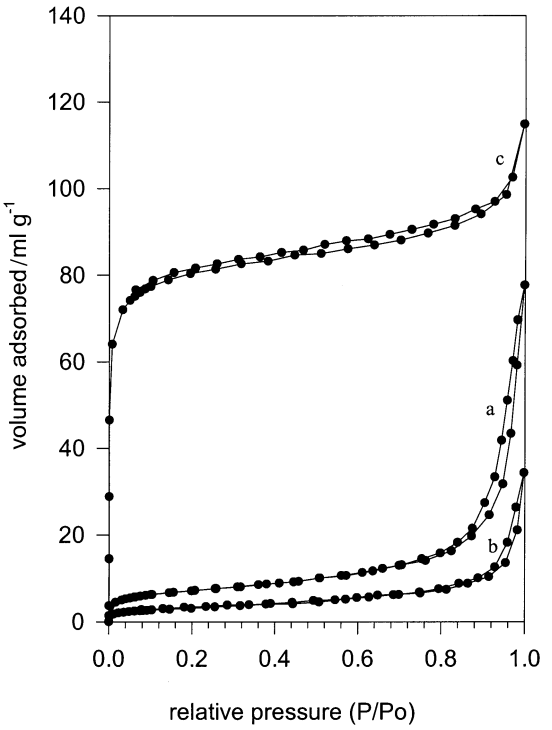

Fig. 8 Nitrogen adsorption–desorption isotherms of (a) Na-magadiite, (b) KLS2 and (c) FLS phases calcined at 500 °C.

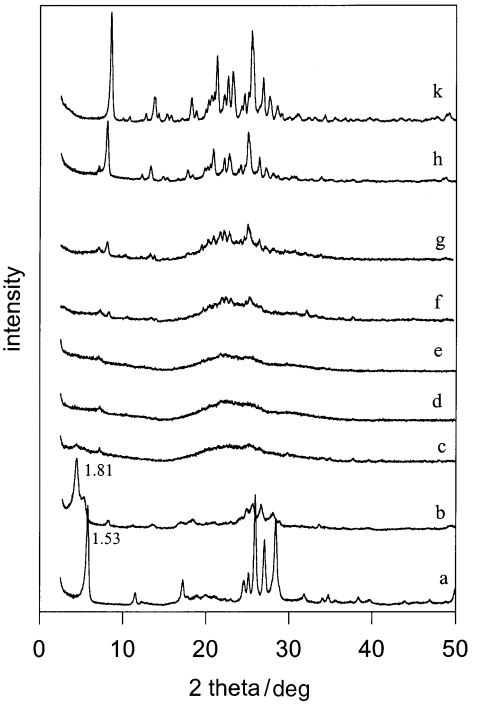

Fig. 9 Powder XRD patterns of (a) Na-magadiite and resulting products after reaction in TMAOH and water, at 170 °C for different times: (b) 1, (c) 2, (d) 4, (e) 6, (f) 8, (g) 9, (h) 10 and (k) 24 h.

Table 3 Surface area and micropore volume of different phases calcined at 500 °C

Sample	S_{BET}/ $m^2\ g^{-1}$	C_{BET}	Micropore volume/mL g^{-1}	C^*_{BET}[a]	S_{ext}/ $m^2\ g^{-1}$
Na-magadiite	25	139	—[b]	139	25
100 °C (5 days)	16	162	—[b]	162	16
150 °C (5 days)	12	132	—[b]	132	12
170 °C (5 days)	300	−235	0.082	100	92
180 °C (5 days)	193	−125	0.043	225	80
190 °C (5 days)	8	145	—[b]	145	8

[a] C^*_{BET} calculated after subtraction of the micropore volume. [b] Negligible.

was used as organic solvent in the reaction mixture.[22,28] The effect of Na cations on complete recrystallization of the latter FLS phase to the KLS2 one is not yet clear. Nevertheless, the structure-directing role of alkali ions in general, and Na in particular, has been well documented.[18c,46] The Na cations are a necessary structure-directing agent in the present case for the formation of the KLS2 phase.

At 170 °C, however, Na-magadiite was converted to the FLS phase. We have tried to study the conversion process at short reaction times (on the order of hours). The powder XRD patterns of the resulting products are presented in Fig. 9. TMA cations are intercalated between magadiite layers following 1 h of reaction, the formation of an amorphous phase after 2 h is due to collapse of TMA-intercalated magadiite. Partial recrystallization of the amorphous phase is observed after 4 h and is complete after 9 h. Further increasing the reaction time leads to an improvement in FLS crystallinity. Although Na cations are present in the reaction mixture they do not take part in the formation of the final product, even after a longer duration of 10 days.

The transformation of the layered silicate to a three-dimensional network *via* intercalation opens up a wide range of possible manipulations for the precursor and might represent a new and more general route to novel porous silicas.

Acknowledgements

F. K. gratefully thanks the New Energy and Industrial Technology Development Organization (NEDO), Japan, for financial support as a NEDO fellow. We thank Dr S. Newman (London College, UK) for his suggestions during the preparation of the manuscript and Dr K. Fujimoto (National Institute for Materials Science, Tsukuba) for his help during the measurement of infra-red spectra.

References

1 G. Lagaly, K. Beneke and A. Weiss, *Am. Mineral.*, 1975, **60**, 642.
2 R. A. Fletcher and D. M. Bibby, *Clays Clay Miner.*, 1987, **35**, 318.
3 G. C. Almond, R. K. Harris and K. R. Franklin, *J. Mater. Chem.*, 1997, **7**, 681.
4 G. C. Almond, R. K. Harris and K. R. Franklin, *J. Mater. Chem.*, 1996, **6**, 843.
5 T. J. Pinnavaia, I. D. Johnson and M. Lipsicas, *J. Solid State Chem.*, 1986, **63**, 118.
6 J. S. Dailey and J. T. Pinnavaia, *J. Inclusion Phenom.*, 1992, **13**, 47.
7 F. Agnes, K. Imre, S. Niwa, M. Toba, Y. Kiyozumi and F. Mizukami, *Appl. Catal., A*, 1999, **176**, L153.
8 C. S. Kim, D. M. Yates and P. J. Heaney, *Clays Clay Miner.*, 1997, **45**, 881.
9 G. Lagaly, *Adv. Colloid Interface Sci.*, 1979, **11**, 105.
10 T. Yanagisawa, C. Yokoyama, K. Kuroda and C. Kato, *Bull. Chem. Soc. Jpn.*, 1990, **63**, 47.
11 Z. Wang and T. J. Pinnavaia, *Chem. Mater.*, 1998, **10**, 1820.
12 S. Inagaki, Y. Fukushima and K. Kuroda, *J. Chem. Soc., Chem. Commun.*, 1993, 680.
13 K. Kuroda, *J. Porous Mater.*, 1996, **3**, 107.
14 C. Y. Chen, S. Q. Xiao and M. E. Davis, *Microporous Mater.*, 1995, **4**, 1.
15 G. Pál-Borbély, H. K. Beyer, Y. Kiyozumi and F. Mizukami, *Microporous Mater.*, 1997, **11**, 45.
16 S. Shimuzi, Y. Kiyozumi, K. Maeda, F. Mizukami, G. Pál-Borbély, R. Magdolna Mihalyi and H. K. Beyer, *Adv. Mater.*, 1996, **8**, 759.

17 M. Salou, Y. Kiyozumi, F. Mizukami and F. Kooli, *J. Mater. Chem.*, 2000, **10**, 2587.
18 (*a*) D. Hasha, L. Sierra de Saldariaga, C. Saldariaga, P. E. Hathaway, D. F. Cox and M. E. Davis, *J. Am. Chem. Soc.*, 1998, **110**, 2127; (*b*) Ch. Baerlocher and W. M. Meier, *Helv. Chim. Acta*, 1969, **52**, 1853; (*c*) B. M. Lok, T. R. Cannan and C. A. Messina, *Zeolites*, 1983, **3**, 282; (*d*) R. Szostak and T. L. Thomas, *J. Chem. Soc., Chem. Commun.*, 1986, 113; (*e*) M. A. Camblor, R. F. Lobo, H. Koller and M. E. Davis, *Chem. Mater.*, 1994, **6**, 2193; (*f*) R. H. Jarman, M. T. Melchior and D. E. W. Vaughan, *ACS Symp. Ser.*, 1983, **218**, 267; (*g*) P. D. Hopkins, *ACS Symp. Ser.*, 1989, **398**, 152; (*h*) L. Sierra de Saldariaga, C. Saldariaga and M. E. Davis, *J. Am. Chem. Soc.*, 1987, **109**, 2686; (*k*) J. M. Newsam and D. E. W. Vaughan, *Stud. Surf. Sci. Catal.*, 1986, **28**, 457; (*l*) F. G. Dwyer and P. Chu, *J. Catal.*, 1979, **59**, 263; (*i*) R. H. Jarman, A. J. Jacobson and M. T. Melchior, *J. Phys. Chem.*, 1984, **88**, 5748.
19 M. Wiebcke and D. Hoebbel, *J. Chem. Soc., Dalton Trans.*, 1992, 2451.
20 M. Wiebcke, J. Emmer and J. Flesche, *Microporous Mater.*, 1995, **4**, 149.
21 D. F. Shantz and R. F. Lobo, *Microporous Mesoporous Mater.*, 2001, **43**, 127.
22 Y. Akiyama, F. Mizukami, Y. Kiyozumi, K. Maeda, H. Izutsu and K. Sakaguchi, *Angew. Chem., Int. Ed.*, 1999, **38**, 1420.
23 T. Ikeda, Y. Akiyama, F. Izumi, Y. Kiyozumi, F. Mizukami and T. Kodaira, *Chem. Mater.*, 2001, **13**, 1286.
24 F. Kooli, Y. Kiyozumi and F. Mizukami, *ChemPhysChem.*, 2001, **8**–**9**, 549.
25 H. P. Eugster, *Science*, 1967, **157**, 1177.
26 G. W. Brindley, *Am. Mineral.*, 1969, **54**, 1583.
27 J. M. Graces, S. C. Rocke, C. E. Crowder and D. L. Hasha, *Clays Clay Miner.*, 1988, **36**, 409.
28 F. Kooli, F. Mizukami, Y. Kiyozumi and Y. Akiyama., *J. Mater. Chem.*, 2001, **11**, 1946.
29 R. Millini, G. Perego, W. O. Parker, Jr. G. Bellussi and L. Carluccio, *Microporous Mater.*, 1995, **4**, 221.
30 M. A. Camblor, R. F. Lobo, H. Koller and M. E. Davis, *Chem. Mater.*, 1994, **6**, 2193.
31 E. M. Flanigen, H. Khatami and H. A. Szymanski, *Adv. Chem. Ser.*, 1971, **101**, 201.
32 J. M. Rojo, E. Ruiz-Hitzky and J. Sanz, *Inorg. Chem.*, 1988, **27**, 2785.
33 Y. Huang, Z. Jiang and W. Schwieger, *Chem. Mater.*, 1999, **11**, 1210.
34 R. Szostak, *Molecular Sieves: Principles of Synthesis and Identification*, Van Nostrand Reinhold, New York, 1989, pp. 323–326.
35 J. C. Jansen, F. J. Van der Gaag and H. Van Bekkum, *Zeolites*, 1984, **4**, 369.
36 A. Zecchina, S. Bordiga, G. Spoto, L. Marchese, G. Petrini, G. Loefanti and M. Padovan, *J. Phys. Chem.*, 1992, **96**, 4985.
37 M. Decottignies, J. Phalippon and J. Zarzycki, *J. Mater. Sci.*, 1978, **13**, 2605.
38 M. R. Boccuti, K. M. Rao, A. Zecchina, G. Leofanti and G. Petrini, *Stud. Surf. Sci. Catal.*, 1989, **48**, 133.
39 G. Coudurier, C. Naccache and J. C. Vedrine, *J. Chem. Soc., Chem. Commun.*, 1982, 1413.
40 G. M. Roe, M. J. Kidd, K. J. Cavell and F. P. Larkin, *Stud. Surf. Sci. Catal.*, 1988, **36**, 509.
41 K. S. W. Sing, D. H. Everett, R. A. W. Paul, L. Moscou, R. A. Pierotti, T. Rouquerol and T. Siemienewska, *Pure Appl. Chem.*, 1985, **57**, 603.
42 A. Gervasini, *Appl. Catal., A*, 1999, **180**, 71.
43 P. J. Branton, K. S. W. Sing and J. W. White, *J. Chem. Soc., Faraday Trans.*, 1997, **93**, 2337.
44 M. J. Remy, A. C. Vieira Coelho and G. Poncelet, *Microporous Mater.*, 1996, **7**, 28.
45 F. Kooli, T. Sasaki, M. Watanabe, C. Martin and V. Rives, *Langmuir*, 1999, **15**, 1090.
46 E. M. Flanigen, *Adv. Chem. Ser.*, 1973, **121**, 119.